

New measures to test modified gravity cosmologies

Jiro Matsumoto,^{a,b,1} Teppei Okumura,^{c,d} and Misao Sasaki^{b,d,e}

^aWind Energy Institute of Tokyo, Inc., Kawate Bld. Suite 501, 1-5-8 Nishi-Shinbashi, Minato-Ku, Tokyo 105-0003, Japan

^bLeCosPA, National Taiwan University, Taipei 10617, Taiwan

^cAcademia Sinica Institute of Astronomy and Astrophysics (ASIAA), No. 1, Section 4, Roosevelt Road, Taipei 10617, Taiwan

^dKavli Institute for the Physics and Mathematics of the Universe (WPI), UTIAS, The University of Tokyo, Kashiwa, Chiba 277-8583, Japan

^eYukawa Institute for Theoretical Physics, Kyoto University, Kyoto 606-8502, Japan

E-mail: ushirugapen@gmail.com, tokumura@asiaa.sinica.edu.tw, misao.sasaki@ipmu.jp

Abstract. The observed accelerated expansion of the Universe may be explained by dark energy or the breakdown of general relativity (GR) on cosmological scales. When the latter case, a modified gravity scenario, is considered, it is often assumed that the background evolution is the same as the Λ CDM model but the density perturbation evolves differently. In this paper, we investigate more general classes of modified gravity, where both the background and perturbation evolutions are deviated from those in the Λ CDM model. We introduce two phase diagrams, $\alpha-f\sigma_8$ and $H-f\sigma_8$ diagrams; H is the expansion rate, $f\sigma_8$ is a combination of the growth rate of the Universe and the normalization of the density fluctuation which is directly constrained by redshift-space distortions, and α is a parameter which characterizes the deviation of gravity from GR and can be probed by gravitational lensing. We consider several specific examples of Horndeski's theory, which is a general scalar-tensor theory, and demonstrate how deviations from the Λ CDM model appears in the $\alpha-f\sigma_8$ and $H-f\sigma_8$ diagrams. The predicted deviations will be useful for future large-scale structure observations to exclude some of the modified gravity models.

Keywords: dark energy, modified gravity, redshift surveys, gravitational lensing

ArXiv ePrint: [2005.xxxxx](https://arxiv.org/abs/2005.xxxxx)

¹Corresponding author.

Contents

1	Introduction	1
2	Dark energy and modified gravity	2
3	More general modified gravity models	4
4	Specific examples	5
4.1	Linear potential, minimally coupled with gravity	6
4.2	Flat potential, non-minimally coupled with gravity	7
4.3	Quadratic potential, non-minimally coupled gravity	8
4.4	Non-canonical kinetic term	8
5	conclusion	9
A	Horndeski's theory	10
B	Possibility of $\alpha < 0$	12

1 Introduction

The accelerated expansion of the current Universe has been clarified by the observations of type Ia supernovae in the late 1990s [1, 2] and supported by observations of cosmic microwave background radiation (CMB) [3–5] and baryon acoustic oscillations (BAO) [6–12]. Broadly speaking, there are two approaches to explain the accelerating Universe; (i) introducing an additional energy component, called dark energy, to the total energy budget and (ii) modifying the action of gravity from the one predicted by Einstein's theory of relativity. In dark energy models, one adopts the Einstein-Hilbert action and introduces a fluid matter with the equation-of-state parameter $w < -1/3$, where $w = -1$ corresponds to a cosmological constant. The simplest dark energy model is Λ CDM, and more generally, the w CDM or quintessence model has been considered [13–16]. On the other hand, the Einstein-Hilbert action itself is modified in the models of modified gravity theories. The models include $F(R)$ gravity [17–21], massive gravity [22–24], and Horndeski's theory [25].

The differences of the models appear both in the background equations and in the linear perturbation equations. While Λ CDM is consistent with most of the observations, a tension between the values of the Hubble constant, H_0 , constrained from early universe and late universe started to be recognized after the Planck mission reported the first results [4]. The discrepancy in the H_0 values between local observations and CMB observations was first reported using Cepheid variables [26–28], and it has also been seen in the observations of strong lensing time delay and so on [29–34]. Moreover, there is another tension in a parameter, $f\sigma_8$, where f is the growth rate of the universe and σ_8 is the normalization of the density fluctuation amplitude. This parameter can be directly constrained through peculiar velocities of galaxies in galaxy redshift surveys, known as redshift-space distortions (RSD) [35, 36], and is used to distinguish modified gravity models [37–41]. However, the $f\sigma_8$ values observed so far at $z < 1$ are systematically lower than the prediction of the best-fitting Λ CDM model from the Planck result [42–47], as pointed out by, e.g., Refs. [48, 49]. Therefore, the importance of reconsidering the dynamics of the Universe in modified gravity models is increasing.

Modified gravity theories, in general, have too many degrees of freedom to be completely analyzed. Consequently, the observables of perturbation quantities (e.g. growth rate of the matter density perturbation) have been investigated only for simple models or for phenomenologically parametrized models. Moreover, the background evolution in modified gravity models is often assumed to be the same as that in the Λ CDM model. In this paper we take account of both the variations of background dynamics and those of perturbation quantities. For this purpose, we introduce new phase diagrams;

the $\alpha-f\sigma_8$ and $H-f\sigma_8$ diagrams. Here α describes the effect on gravitational lensing and is defined in Eq. (2.4) below in terms of the deflection potential Φ_{defl} , and $\alpha = 0$ in the case of general relativity (e.g., [50–55]). Thus, these diagrams will enable us to investigate how each of the two key observations of large-scale structures, RSD and gravitational lensing, can constrain a given modified gravity model.

In this paper, we consider Horndeski’s theory, which is a general scalar-tensor theory. We do not adopt phenomenological parameterizations which have been commonly used in the literature. We focus several specific examples of Horndeski’s gravity and demonstrate how deviations from the Λ CDM model appear in the $\alpha-f\sigma_8$ and $H-f\sigma_8$ diagrams.

The contents of the paper are as follows. We briefly overview how models of dark energy and modified gravity behave on the $\alpha-f\sigma_8$ and $H-f\sigma_8$ diagrams in Sec. 2. For this purpose we present the former and latter diagrams for the simple representative cases of dark energy and modified gravity, the w CDM and $F(R)$ gravity models, respectively. Then we describe Horndeski’s theory in Sec. 3, and considering its typical examples, we present their $\alpha-f\sigma_8$ and $H-f\sigma_8$ diagrams in Sec. 4. Our concluding remarks are given in Sec. 5. A more detailed description of Horndeski’s theory is presented in Appendix A. A short note on the possibility of having negative α is given in Appendix B.

Throughout this paper, we adopt Natural units, $\hbar = c = k_B = 1$, and the gravitational constant $8\pi G$ is denoted by $\kappa^2 \equiv 8\pi/M_{Pl}^2$ with the Planck mass of $M_{Pl} = G^{-1/2} = 1.2 \times 10^{19}$ GeV.

2 Dark energy and modified gravity

In models in which dark energy is given by a matter field, commonly its energy momentum tensor is decoupled from the other matter components. In this case, the main effect of dark energy is to modify the background evolution of the Universe, and hence its effect to the growth of linear perturbations is indirect. On the other hand, in modified gravity theories of dark energy, its effective energy momentum tensor is likely to be coupled to the matter components. As a result, not only the background evolution of the Universe but also the linear perturbation equations may significantly deviate from those in the Λ CDM model.

In the following, we assume the metric,

$$ds^2 = -(1 + 2\Psi(t, x))dt^2 + a^2(t)(1 + 2\Phi(t, x))\delta_{ij}dx^i dx^j, \quad (2.1)$$

and adopt notations in Fourier space as

$$\Psi(t, k) + (1 + \alpha(t, k))\Phi(t, k) = 0, \quad (2.2)$$

$$\delta\rho(t, k)/\rho(t) = \delta(t, k) = \hat{\delta}(k)D(t, k), \quad (2.3)$$

where k is the wave number, $D(t, k)$ is the growing mode of the matter density perturbation, and $\hat{\delta}(k)$ describes the scale dependence of $\delta(t, k)$ at initial time $t = t_i$ under the normalization of D as $D(t_i, k) = 1$.

In Eq. (2.2), we introduced a quantity α , which vanishes in Einstein gravity (i.e., $\Psi + \Phi = 0$). Thus α characterizes how much a given gravity model deviates from General Relativity (GR). Because the strength of gravitational lensing is determined by the deflection potential [56],

$$\Phi_{\text{defl}} \equiv \Psi - \Phi = \frac{2 + \alpha}{1 + \alpha}\Psi = \left(2 - \frac{\alpha}{1 + \alpha}\right)\Psi, \quad (2.4)$$

we see that the gravitational lensing effect is reduced if $\alpha > 0$ or $\alpha < -2$ and enhanced if $-2 < \alpha < 0$. We note that there is a subtlety in this interpretation. It will be shown in section 4 that, for a class of modified gravity models considered in this paper, the lensing effect is unaffected if we compare it for the same mass distribution. Namely, if we take into account the effect on the effective gravitational constant in modified gravity, one obtains

$$G_{\text{eff}} = \frac{2(1 + \alpha)}{2 + \alpha}G, \quad (2.5)$$

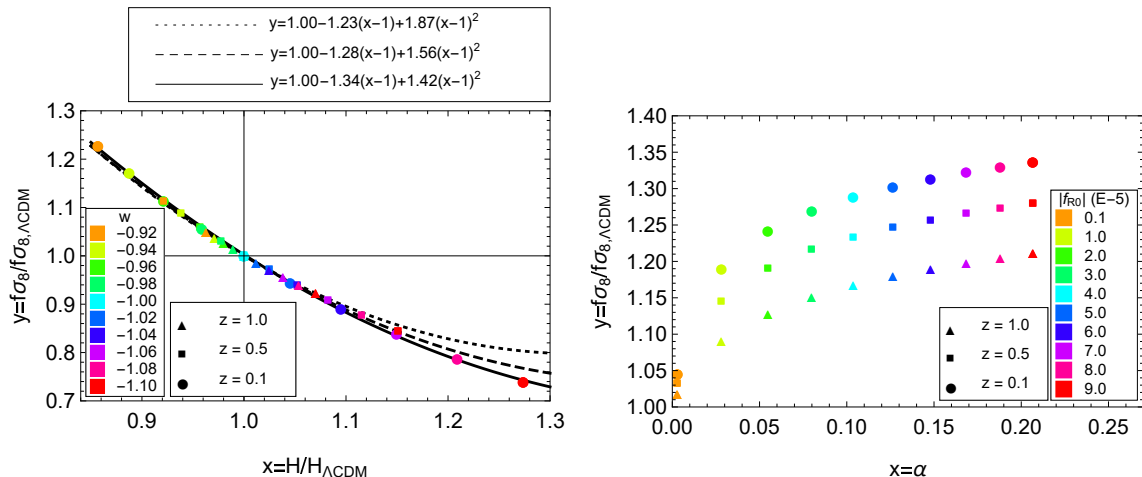


Figure 1. (Left) $H-f\sigma$ diagram for the w CDM model for various values of the equation of state parameter w . Dark matter density is set to be the same as that in the Λ CDM model. Triangles, Squares, and Circles correspond to redshift 1.0, 0.5, and 0.1, respectively. In order to clarify the redshift dependences, the best-fitting quadratic curves are shown for the redshifts 1.0 (dotted), 0.5 (dashed) and 0.1 (solid).

Figure 2. (Right) $\alpha-f\sigma_8$ diagram for the $F(R)$ gravity model with $F(R) = R - 2\Lambda + |f_{R0}|R_0^2/R$ for various values of $|f_{R0}|$.

implying that the resulting Φ_{def} will be the same as that in GR, independent of α . However, as the mass distribution is measured by its gravitational effect that includes the modification in the effective gravitational constant, what can be compared is the lensing effect for the same Ψ . This means our original interpretation is correct from an observational point of view. More precisely speaking, it is the gravitationally inferred mass distribution that is overestimated if $\alpha > 0$ or $\alpha < -2$ and otherwise if $-2 < \alpha < 0$, while the gravitational lensing effect remains the same.

To quantify the growth of linear perturbations, one usually considers the combination, $f\sigma_8$, inferred from galaxy surveys, where $f = d \ln D / d \ln a$ and σ_8 is the normalization parameter of the density perturbation spectrum. In the following, to test modified gravity models, we evaluate the ratio of $f\sigma_8$ in a given model to that in the Λ CDM model, $f\sigma_8/f\sigma_{8,\Lambda\text{CDM}}$. Note that the value of f should approach unity in any viable model of gravity in the high-redshift limit. We also assume that the value of σ_8 coincides with that of the Λ CDM model in the high redshift limit. Thus, this ratio becomes unity at high redshifts. Since $f\sigma_8$ depends not only on the modifications of the linear perturbation equations but also on the background evolution of the Universe, below we will study correlations between $f\sigma_8$ and α and between $f\sigma_8$ and the Hubble expansion rate H in various models of gravity.

Before presenting detailed studies on modified gravity models, let us first consider the simplest dark energy model, i.e. the w CDM model. Note that $\alpha = 0$ because there is no deviation from GR in this model. The $H-f\sigma_8$ diagram is depicted in Fig. 1. The initial conditions are set at $z = 10$ where they coincides with those of the Λ CDM model. The figure shows that the deviation in $f\sigma_8$ is almost proportional to that in the Hubble rate at each redshift, with negative proportionality coefficients. Thus $f\sigma_8$ in w CDM models becomes smaller than that in the Λ CDM model for models with a larger Hubble rate H which corresponds to $w < -1$. We note that the linear perturbation equations in the w CDM model are unchanged from those of the Λ CDM model. Therefore, the smaller value of $f\sigma_8$ due to a larger H may be regarded as a purely background effect. We should note that if we apply a different boundary condition, e.g., $H_{w\text{CDM}} = H_{\Lambda\text{CDM}}$ and $\Omega_m = 0.31$ at $z = 0$, the quantitative results will be different though the qualitative tendency will remain the same.

As we mentioned in the above, the behavior of the matter density perturbation is not independent from the background evolution of the Universe in general. In some theories, e.g. $F(R)$ gravity theories,

even if the difference between the model and GR at the background level is negligibly small, there can be $O(1)$ difference at perturbation level due to the scale dependence of the matter density perturbation that enhances the deviation from GR on small scales. As a characteristic example for such a case, let us consider $F(R)$ gravity with

$$F(R) = R - 2\Lambda + |F_{R0}| \frac{R_0^2}{R}, \quad (2.6)$$

where R_0 and Λ are the current values of the Ricci scalar and the cosmological constant, respectively. For the parameter F_{R0} in the range $10^{-6} < |F_{R0}| < 10^{-4} \ll \Lambda/R_0$, this model is known to reproduce the background evolution of the Λ CDM model almost exactly [57]. In Fig. 2, we plot the predicted values of α and $f\sigma$ for several redshifts. In general, the function $\delta(t, k)$ is not separable, in the other words, the k -dependence of $D(t, k)$ in (2.3) cannot be ignored in $F(R)$ gravity theories. Here, for definiteness, we plot $f\sigma_8$, i.e. $f\sigma$ at $k = (8h^{-1}\text{Mpc})^{-1}$. It shows that the density perturbation in this model always evolves faster than that in the case of the Λ CDM model, and α is always positive.

3 More general modified gravity models

In the previous section, we studied two examples; w CDM model and $F(R)$ gravity theory. In the w CDM case, the linear perturbation equations are the same as those in the Λ CDM model, while the background evolution of the Universe is different. On the other hand, in the $F(R)$ gravity case, the background evolution of the Universe is the same as the Λ CDM model, while the linear perturbation equations are different. In more general modified gravity theories, both of them will be different from the Λ CDM model. Here we consider Horndeski's theory. It is a general scalar-tensor theory which includes $F(R)$ gravity as a special case [58–60].

The action in Horndeski's theory is given by [25, 61, 62]

$$S_H = \sum_{i=2}^5 \int d^4x \sqrt{-g} \mathcal{L}_i, \quad (3.1)$$

where

$$\mathcal{L}_2 = K(\phi, X), \quad (3.2)$$

$$\mathcal{L}_3 = -G_3(\phi, X) \square \phi, \quad (3.3)$$

$$\mathcal{L}_4 = G_4(\phi, X) R + G_{4X} [(\square \phi)^2 - (\nabla_\mu \nabla_\nu \phi)^2], \quad (3.4)$$

$$\mathcal{L}_5 = G_5(\phi, X) G_{\mu\nu} \nabla^\mu \nabla^\nu \phi - \frac{G_{5X}}{6} [(\square \phi)^3 - 3(\square \phi)(\nabla_\mu \nabla_\nu \phi)^2 + 2(\nabla_\mu \nabla_\nu \phi)^3]. \quad (3.5)$$

Here, K , G_3 , G_4 , and G_5 are generic functions of ϕ and $X = -\partial_\mu \phi \partial^\mu \phi / 2$, and the subscript X means a derivative with respect to X . The total action is the sum of S_H and the matter action S_{matter} which contains baryons and cold dark matter. More details are referred to Appendix A

The recent observations of gravitational wave event GW170817 [63] and its electromagnetic counterparts [64–66] showed that the propagation speed of gravitational waves should satisfy

$$|c_T^2 - 1| \lesssim 10^{-15}, \quad (3.6)$$

in the relatively recent Universe. This bound implies the sound speed of the tensor mode, given by

$$c_T^2 = \frac{G_4 - XG_{5\phi} - XG_{5X}\ddot{\phi}}{G_4 - 2XG_{4X} - X(G_{5X}\dot{\phi}H - G_{5\phi})}, \quad (3.7)$$

should be almost unity, where and below the subscript ϕ means a derivative with respect to ϕ . If the terms $XG_{5\phi}$, XG_{4X} , \dots are relevant for the evolution of the Universe, then one expects a substantial deviation of c_T^2 from unity. Therefore, it is reasonable to assume that the terms proportional to G_{4X} ,

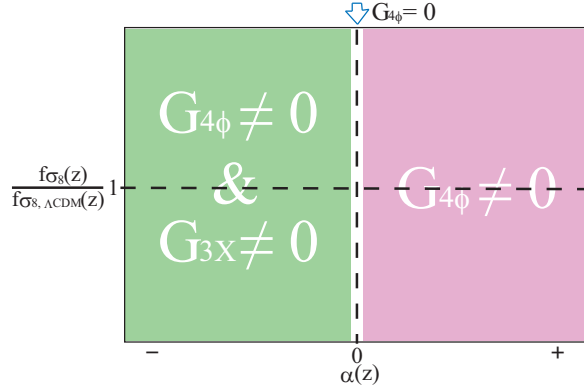


Figure 3. Classification of Horndeski's models in terms of α and f under the assumptions $K_X > 0$ and $G_4 > 0$. Nonzero α is only realized when $G_{4\phi} \neq 0$, and $\alpha < 0$ is realized only if $G_{4\phi} \neq 0$ and $G_{3X} \neq 0$.

$G_{5\phi}$, and G_{5X} are not relevant for the current accelerated expansion of the Universe. Hence we set $G_{4X} = G_5 = 0$ in the following.

Even after this simplification, the theory still remains quite complicated. For example, the effective Newton constant that can be defined on sufficiently small scales $k^2 \gg a^2 H^2$ takes the form [55],

$$G_{\text{eff}} = \frac{1}{16\pi G_4} \left(\frac{\mathcal{A}}{\mathcal{B}} + O(a^2 H^2/k^2) \right); \quad (3.8)$$

$$\mathcal{A} \equiv G_4 C_{\text{kin}} + 4G_{4\phi}^2, \quad (3.9)$$

$$\mathcal{B} \equiv G_4 C_{\text{kin}} - \frac{1}{4} \dot{\phi}^4 G_{3X}^2 - \dot{\phi}^2 G_{3X} G_{4\phi} + 3G_{4\phi}^2, \quad (3.10)$$

where we have introduced an effective coefficient of the kinetic term C_{kin}

$$C_{\text{kin}} = K_X - 2G_{3\phi} + \ddot{\phi}(2G_{3X} + \dot{\phi}^2 G_{3XX}) + \dot{\phi}^2 G_{3\phi X} + 4H\dot{\phi}G_{3X}. \quad (3.11)$$

As for α which describes the modification of the lensing effect, it is expressed using Eq. (3.11) as [55]

$$\alpha = \frac{G_{4\phi}(2G_{4\phi} + \dot{\phi}^2 G_{3X})}{G_4 C_{\text{kin}} + G_{4\phi}(-\dot{\phi}^2 G_{3X} + 2G_{4\phi}) + O(a^2 H^2/k^2)}. \quad (3.12)$$

The above equation shows that α is non-vanishing only if G_4 is non-trivial, i.e. is ϕ -dependent. It also shows that $\alpha < 0$ is realized only if $G_{3X} \neq 0$ provided that we have $K_X > 0$ and $G_4 > 0$ which are satisfied for most healthy theories of gravity (see Fig. 3). Thus $\alpha = 0$ if $G_{4\phi} = 0$, $\alpha > 0$ if $G_{4\phi} \neq 0$ and $G_3 = 0$, while α can be positive or negative if $G_3 \neq 0$ and $G_{4\phi} \neq 0$.

In passing we note that $f(R)$ gravity theories correspond to the case [58–60];

$$K = \frac{M_{\text{pl}}^2}{16\pi}(F - RF_{,R}), \quad G_3 = G_5 = 0, \quad G_4 = \frac{1}{2\sqrt{8\pi}}M_{\text{pl}}\phi, \quad \phi = \frac{1}{\sqrt{8\pi}}M_{\text{pl}}F_{,R}. \quad (3.13)$$

Because $G_3 = 0$, α is always positive in $f(R)$ gravity with $K_X > 0$. We should note that $O(a^2 H^2/k^2)$ terms in Eqs. (3.8) and (3.12) are to be taken into account in $F(R)$ gravity models [58]. The case $K_X \leq 0$ with $G_3 = 0$ or $K_X - 2G_{3\phi} \leq 0$ may be also acceptable if instabilities are absent. Such a case is discussed in Appendix B, but we will not consider it in the main text for simplicity.

4 Specific examples

Let us now consider a few specific examples of Horndeski's gravity that show small but observationally interesting deviations from the Λ CDM model. To compare with the Λ CDM model, we will assume

the same amount of dark matter as that in the Λ CDM model and fix the ratio $f\sigma_8/\Lambda\text{CDM}/f\sigma_8 = 1$ at sufficiently high redshifts, $z \geq 10$. In what follows, to evaluate the effects of functions $K(\phi, X)$, $G_3(\phi, X)$, and $G_4(\phi)$, we assume their forms as

$$K(\phi, X) = X + K_2 X^2 - (V_0 + V_1 \phi + m^2 \phi^2), \quad (4.1)$$

$$G_3(\phi) = g\phi, \quad (4.2)$$

$$G_4(\phi) = \frac{1}{2\kappa^2} \exp\left[\lambda \frac{\phi}{M_{pl}}\right], \quad (4.3)$$

where K_2 , V_0 , V_1 , m^2 , g and λ are constant parameters.

In this above class of models, the expressions for α and G_{eff} are greatly simplified as

$$\alpha = \frac{2G_{4\phi}^2}{G_4 C_{\text{kin}} + 2G_{4\phi}^2}, \quad (4.4)$$

$$G_{\text{eff}} = \frac{G_4 C_{\text{kin}} + 4G_{4\phi}^2}{16\pi G_4 (G_4 C_{\text{kin}} + 3G_{4\phi}^2)}, \quad (4.5)$$

where C_{kin} defined in Eq. (3.11) is also simplified as

$$C_{\text{kin}} = K_X - 2G_{3\phi}. \quad (4.6)$$

As $G_{4\phi}$ should be small enough to guarantee the proximity to Newton gravity in the large scale structure formation, the above two equations imply that α is small and positive if $C_{\text{kin}} = O(1)$ and > 0 , and $G_{\text{eff}} \approx G$.

Now we are in a position to evaluate the effect of α on gravitational lensing for the same mass density distribution. Since the resulting gravitational potential is proportional to the effective gravitational constant G_{eff} , the resulting gravitational lensing effect is proportional to the deflection potential given by

$$\Phi_{\text{defl}} = \frac{2 + \alpha}{1 + \alpha} \Psi = \frac{2 + \alpha}{1 + \alpha} \frac{G_{\text{eff}}}{G} \Psi_{GR}, \quad (4.7)$$

where Ψ_{GR} is the gravitational potential of the mass distribution if gravity were GR. Using Eqs. (4.4) and (4.5), we find

$$G_{\text{eff}} = \frac{1}{\kappa^2 G_4} \frac{1 + \alpha}{2 + \alpha} G = \frac{1 + \alpha}{2 + \alpha} \exp\left[-\lambda \frac{\phi}{M_{pl}}\right] G, \quad (4.8)$$

which gives

$$\Phi_{\text{defl}} = 2 \exp\left[-\lambda \frac{\phi}{M_{pl}}\right] \Psi_{GR} = \exp\left[-\lambda \frac{\phi}{M_{pl}}\right] \Phi_{\text{defl},GR}, \quad (4.9)$$

where $\Phi_{\text{defl},GR}$ is the deflection potential in the case of GR. Thus we see that the gravitational lensing effect is independent of α for the same mass density distribution. In particular, it remains essentially the same as that in GR if $\lambda\phi/M_{pl} \ll 1$, as we mentioned in section 2.

4.1 Linear potential, minimally coupled with gravity

First we consider the case $K = X - (V_0 + V_1\phi)$ with $G_3 = 0$ and $G_4 = \text{const.}$, which represents a quintessential field [14]. In this case, α always vanishes as seen from Eq. (3.12). Figure 4 shows the correlations between $f\sigma_8$ and H for various values of V_1 at several different redshifts. One sees that a higher Hubble rate is accompanied with a lower growth rate of the matter density perturbation, which is similar to the case of the w CDM model shown in Fig. 1. Note that $\alpha = 0$ also in the w CDM model. These similarities are due to the fact that both models have no non-minimal coupling with gravity.

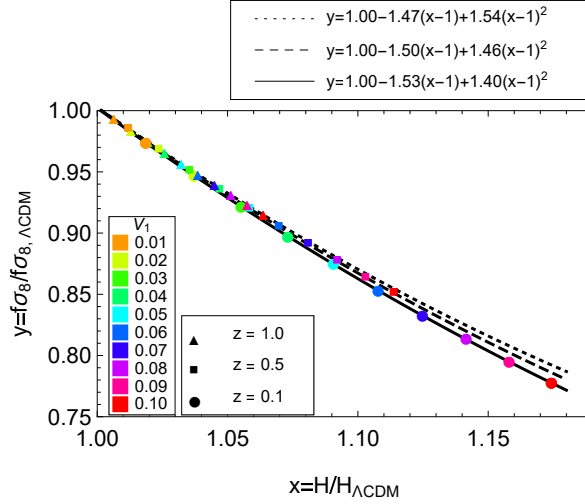


Figure 4. $H-f\sigma_8$ diagram in the case $K = X - (V_0 + V_1\phi)$, $G_3 = 0$ and $G_4 = \text{const.}$ for various of V_1 . The initial conditions are set as $\phi = 0.5M_{pl}$ and $\dot{\phi} = -2V_1/(9H)$ at $z = 10$. The best-fitting quadratic curves are shown for the redshifts 1.0 (dotted), 0.5 (dashed) and 0.1 (solid).

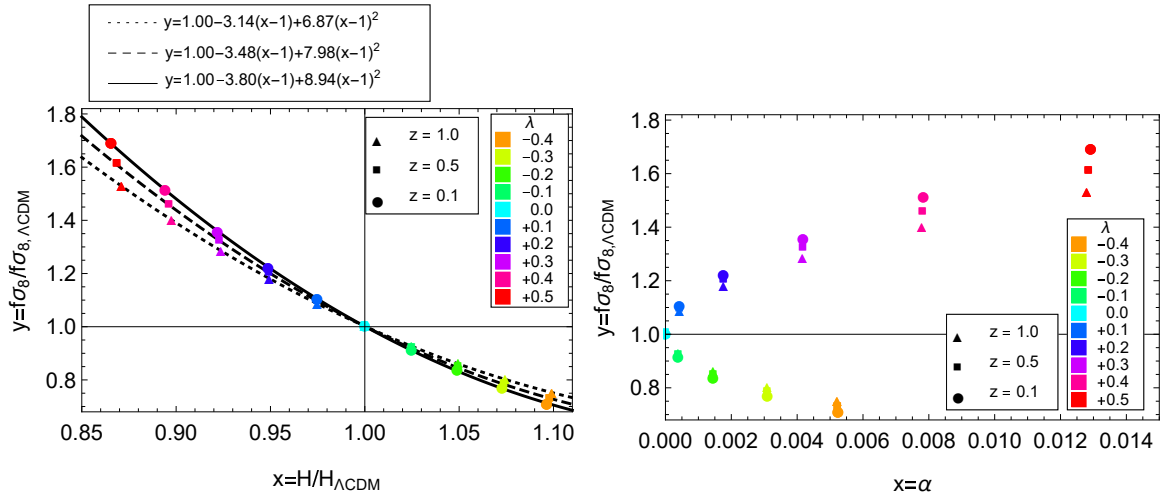


Figure 5. $H-f\sigma_8$ (left) and $\alpha-f\sigma_8$ (right) diagrams for the case $K = X - V_0$, $G_3 = 0$ and $G_4 = \exp[\lambda\phi/M_{pl}]/(2\kappa^2)$ for various values of λ . The initial conditions are $\phi = 0.5M_{pl}$ and $\dot{\phi} = \lambda \exp[\lambda\phi/M_{pl}]/(18\pi H)$ at $z = 10$. In the left panel the best-fitting quadratic curves are shown for the redshifts 1.0 (dotted), 0.5 (dashed) and 0.1 (solid).

4.2 Flat potential, non-minimally coupled with gravity

Next we consider the effect of non-minimal coupling with gravity, namely, the case where $G_4 = \exp[\lambda\phi/M_{pl}]/(2\kappa^2)$ with $K = X - V_0$ and $G_3 = 0$ (e.g., see [67, 68]). Figure 5 shows the correlations between $f\sigma_8$ and H and between $f\sigma_8$ and α . The $H-f\sigma_8$ diagram on the left is similar to that of the minimally coupled linear potential case except for the inclinations of the fitted curves. On the other hand, the $\alpha-f\sigma_8$ diagram is quite different: α is always non-negative as in the case of $F(R)$ gravity, see Fig. 2 while it vanishes in the minimally coupled linear potential case. We also note that the ratio $f\sigma_8/f\sigma_{8,\Lambda\text{CDM}}$ can be greater or smaller than unity depending on the sign of λ in contrast to the $F(R)$ gravity case where the ratio is always greater than unity. The similarity and difference from the $F(R)$ gravity case can be explained by the fact that α does not depend on the sign of λ or

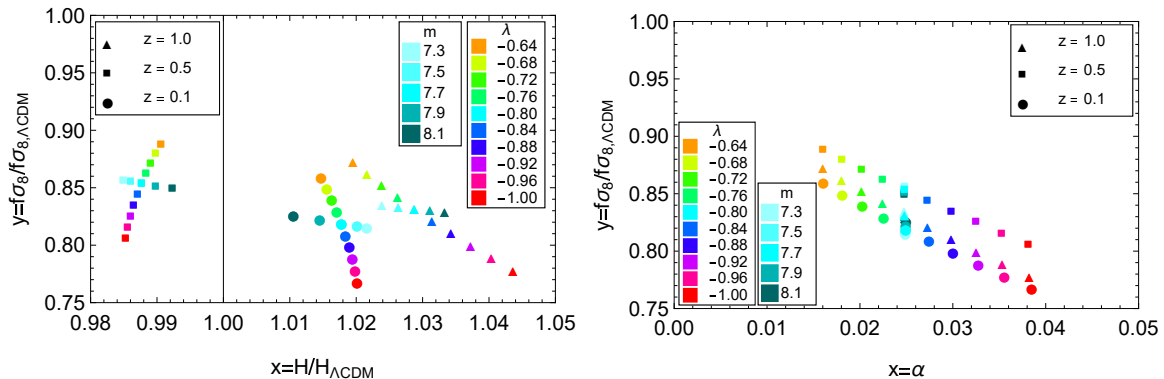


Figure 6. Same as Fig. 5, but for the case $K = X - (V_0 + m^2\phi^2)$, $G_3 = 0$ and $G_4 = \exp[\lambda\phi/M_{pl}]/(2\kappa^2)$. The initial conditions are $\phi = -0.03M_{pl}$ and $\dot{\phi} = 0.04H_0M_{pl}$ at $z = 10$.

$G_{4\phi}$, while G_{eff} may increase or decrease depending on the sign of λ .

4.3 Quadratic potential, non-minimally coupled gravity

The third case we consider is the model which can explain the reconstructed equation-of-state parameter from recent observations [69]. The Lagrangian of the model is given by

$$K = X - (V_0 + m^2\phi^2), \quad G_3 = 0, \quad G_4 = \frac{1}{2\kappa^2}e^{\lambda\phi/M_{pl}}. \quad (4.10)$$

This model is similar to a combination of the models considered in subsections 4.1 and 4.2. However, it differs from such a model in that there is an oscillation of the equation of state parameter induced by the oscillation of the scalar field, which gives rise to an oscillatory evolution in the Hubble rate as can be seen in the left panel of Fig. 6. We find $f\sigma_8$ in this model is always smaller than that in the Λ CDM model even at $z = 0.5$ at which $H/H_{\Lambda\text{CDM}} < 1$. This result may be understood if we note the fact that $f(z) = d \ln D / d \ln a$, which $\sigma_8(z)$ is proportional to, depends non-locally on time, or it is a hysteresis effect of the oscillatory evolution in the present case. We also note that α does not vary much within the range of parameters we adopted, with the values in the range $0.02 \sim 0.04$.

Actually the small positiveness of α is a common feature in models that satisfy $K_X - 2G_{3\phi} = O(1)$ and $G_{4\phi} \neq 0$, provided that the background evolution does not deviate much from that in the Λ CDM model. This may be seen by comparing Eqs. (4.4) and (4.5). If we require $G_{4\phi}$ to be small enough to guarantee the proximity to Newton gravity, namely, $G_{4\phi}^2/G_4 \ll 1$, these two equations implies that α is small and positive if $C_{kin} = O(1)$ and $G_{\text{eff}} \approx G$.

4.4 Non-canonical kinetic term

If we want to consider models with larger values of α and possibly substantial deviations of G_{eff} from Newton gravity, we need to relax the assumption $C_{kin} = K_X - 2G_{3\phi} = O(1)$. From Eq. (3.12), one notices that $\alpha = O(1)$ can be realized if $2G_{4\phi}(\phi)^2 \gg C_{kin}G_4$. Since $K_X = 1$ and $G_3 = 0$ for a canonical scalar field, one has to resort to a non-canonical scalar field model to achieve it. For definiteness, we propose the following model,

$$K(\phi, X) = X + K_2X^2 - V_0, \quad G_3 = \frac{\phi}{2}, \quad (4.11)$$

which gives $C_{kin} = 2K_2X$. For $K_2 = O(H_0^2M_{pl}^2)$, $C_{kin} = O(\dot{\phi}^2/V_0) \ll 1$ for a slowly rolling scalar field. Thus this model can achieve $C_{kin} \ll 1$ and hence $\alpha = O(1)$. Here we focus on the case $K_2 > 0$ because the scalar field would become non-dynamical if $K_2 = 0$ and it would become a ghost if $K_2 < 0$.

Figure 7 shows the $H - f\sigma_8$ and $\alpha - f\sigma_8$ diagrams in this case for various values of K_2 in units of $K_2/(H_0^2M_{pl}^2)$. As seen from the left panel, the background evolution of the Universe is almost same

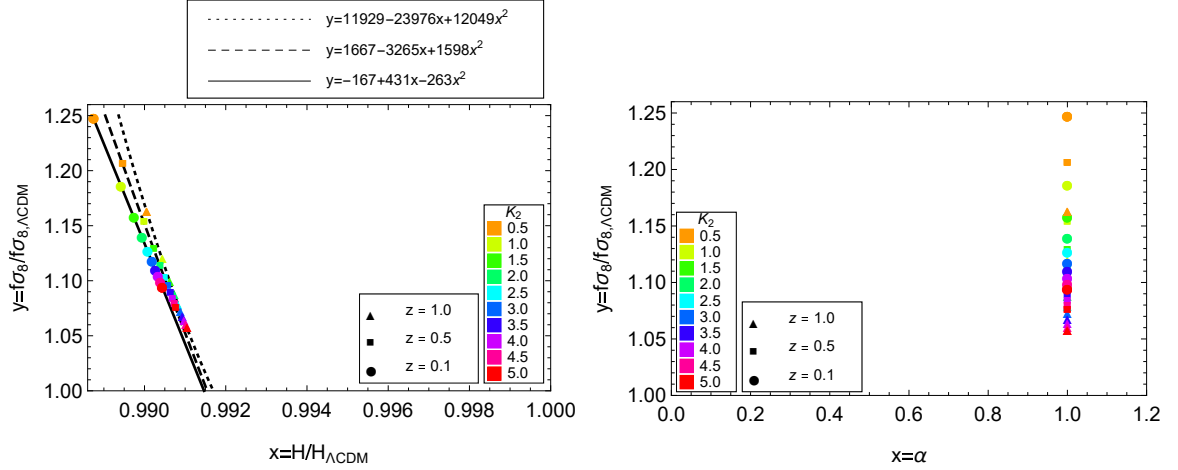


Figure 7. Same as Fig. 5, but for the case $G_3(\phi, X) = \phi/2$ and $K(\phi, X) = X + K_2 X^2 - \Lambda$ for various values of $K_2/(H_0^2 M_{pl}^2)$. The initial conditions are $\phi = 0.5 M_{pl}$ and $\dot{\phi} = 0.4 H_0 M_{pl}$ at $z = 10$.

as that in the ΛCDM , with $f\sigma_8/f\sigma_{8,\Lambda\text{CDM}} > 1$. This behavior is similar to $F(R)$ gravity. The right figure shows that $\alpha = 1$ is certainly realized in this case. $\alpha = 1$ means that the gravitational lensing effect is enhanced by a factor $3/2$. We note that, for a more general form of $C_{kin} = K_X - 2G_{3\phi}$, we may achieve any value of α in the range $0 < \alpha < 1$ while keeping the ΛCDM like background evolution intact. We also note that G_{eff} would substantially deviate from the Newtonian G if $G_4 \approx (2\kappa^2)$ as seen from Eq. (4.8).

5 conclusion

We have investigated a class of dark energy models based on Horndeski's theory of modified gravity which exhibit small but interesting deviations from the ΛCDM model not only in the background evolution but also in the linear perturbation level. The models include the $w\text{CDM}$, $F(R)$ gravity, and four kinds of Horndeski gravity models. To classify the properties of these models, we have introduced two diagrams; $H-f\sigma_8$ and $\alpha-f\sigma_8$ diagrams. We have found that these two diagrams provide a useful tool to distinguish the differences in the observational predictions of different models from each other.

Figure 8 shows the summary of our results. The right panel shows the $\alpha-f\sigma_8$ diagram, which exhibits deviations in the behavior of linear perturbations from GR, at $z = 0.5$ for various models with various parameters. The canonical scalar model with linear potential (denoted by V_1 , discussed in section 4.1) does not have a direct coupling to gravity, hence $\alpha = 0$. The non-minimally coupled scalar model with flat potential (denoted by G_4 , discussed in section 4.2) gives non-vanishing α but the values are too small ($\sim O(0.01)$) to be seen in the figure, whereas the non-minimally coupled scalar model with quadratic potential (denoted by G_4m^2 , discussed in section 4.3). As for the non-minimally coupled scalar model with non-canonical kinetic term (denoted by G_4Kx , discussed in section 4.4), $\alpha = 1$, that is the dynamics of the linear perturbation is quite different from GR.

In all of the models studied in this paper, we have found $\alpha > 0$. As discussed in Appendix B, there exist theoretically acceptable models with negative α , but they all satisfy $\alpha < -2$. In fact, the condition $\alpha < -2$ is necessary to guarantee the positivity of G_{eff} as can be seen from Eq. (4.8). Thus either $\alpha > 0$ or $\alpha < -2$, our result implies that gravity becomes effectively stronger than GR in all the models. In other words, if we are to measure the mass density distribution, we would overestimate it if we use the gravitational dynamics, while we would obtain a correct estimate if we use gravitational lensing observations. Whether this has any substantial implications to observational data analysis is an issue to be studied.

The left panel shows the $H-f\sigma_8$ diagram at $z = 0.5$ for various models with various parameters. It shows the dependence of the growth rate of linear perturbations on the difference in the background

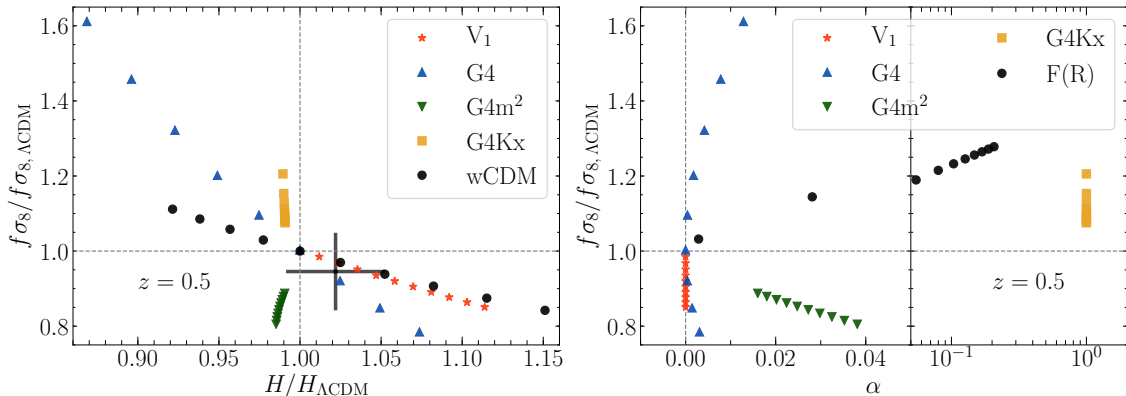


Figure 8. Summary of the $H-f\sigma$ (left) and $\alpha-f\sigma_8$ (right) diagrams for various dark energy models at redshift $z = 0.5$. In the legend, V_1 , G_4 , G_{4m^2} , and G_{4Kx} represent the cases studied in subsections 4.1, 4.2, 4.3, and 4.4, respectively. The w CDM model and $F(R)$ gravity model are also plotted, respectively, in the $H-f\sigma$ diagram and $\alpha-f\sigma_8$ diagram for comparison. The black cross expresses on the left panel 1σ constraint from the observation by Alam *et al.* [70]. Note that the horizontal axis of the right panel mixes linear and logarithmic scales for clarity.

evolution of the Universe. We see that in all models except for the non-minimally coupled scalar model with quadratic potential or non-canonical kinetic term, there is a tendency that larger H gives smaller $f\sigma_8$ in comparison with Λ CDM. In the case of the quadratic potential model (G_{4m^2}), because of the oscillatory feature in H , the fact that $f\sigma_8$ are smaller for smaller H depends on the redshift, as well as on the choice of the model parameters. So it is difficult to discuss a general tendency in this model. In the case of the non-canonical kinetic term model (G_{4Kx}), the dependence of $f\sigma_8$ on H seems very small. This is explained by the fact that this model can mimic the Λ CDM model very well as long as the background evolution of the Universe is concerned.

The blue bars denote observational 1σ error bars obtained by Alam *et al.* [70]. Since it is a 1σ constraint, no reliable conclusion can be drawn, but it seems that when compared to the Λ CDM model, those models that yield slightly larger H with slightly smaller $f\sigma_8$ are preferred.

So far, observational constraints are not so severe yet to exclude any of these models. But eventually we will be able to exclude most of the models as observational accuracies improve. The $H-f\sigma$ and $\alpha-f\sigma_8$ diagrams we introduced, or their variants, may play an important role at such a stage.

Acknowledgments

We would like to thank T. Namikawa for discussions in the early stage of this work. T. O. acknowledges support from the Ministry of Science and Technology of Taiwan under Grants No. MOST 106-2119-M-001-031-MY3 and the Career Development Award, Academia Sinica (AS-CDA-108-M02) for the period of 2019 to 2023. The work of M. S. is supported in part by JSPS KAKENHI No. 20H04727.

A Horndeski's theory

Let us first recapitulate the action in Horndeski's theory [25, 61, 62],

$$S_H = \sum_{i=2}^5 \int d^4x \sqrt{-g} \mathcal{L}_i, \quad (\text{A.1})$$

where

$$\mathcal{L}_2 = K(\phi, X), \quad (\text{A.2})$$

$$\mathcal{L}_3 = -G_3(\phi, X)\square\phi, \quad (\text{A.3})$$

$$\mathcal{L}_4 = G_4(\phi, X)R + G_{4X} [(\square\phi)^2 - (\nabla_\mu\nabla_\nu\phi)^2], \quad (\text{A.4})$$

$$\mathcal{L}_5 = G_5(\phi, X)G_{\mu\nu}\nabla^\mu\nabla^\nu\phi - \frac{G_{5X}}{6} [(\square\phi)^3 - 3(\square\phi)(\nabla_\mu\nabla_\nu\phi)^2 + 2(\nabla_\mu\nabla_\nu\phi)^3]. \quad (\text{A.5})$$

Here, K , G_3 , G_4 , and G_5 are generic functions of ϕ and $X = -\partial_\mu\phi\partial^\mu\phi/2$, and the subscript X means a derivative with respect to X . The total action is the sum of S_H and the matter action S_{matter} .

The Friedman equations are given by [62]

$$\rho_{\text{matter}} + \sum_{i=2}^5 \mathcal{E}_i = 0, \quad (\text{A.6})$$

where

$$\mathcal{E}_2 = 2XK_X - K, \quad (\text{A.7})$$

$$\mathcal{E}_3 = 6X\dot{\phi}HG_{3X} - 2XG_{3\phi}, \quad (\text{A.8})$$

$$\mathcal{E}_4 = -6H^2G_4 + 24H^2X(G_{4X} + XG_{4XX}) - 12HX\dot{\phi}G_{4\phi X} - 6H\dot{\phi}G_{4\phi}, \quad (\text{A.9})$$

$$\mathcal{E}_5 = 2H^3X\dot{\phi}(5G_{5X} + 2XG_{5XX}) - 6H^2X(3G_{5\phi} + 2XG_{5\phi X}), \quad (\text{A.10})$$

and

$$p_{\text{matter}} + \sum_{i=2}^5 \mathcal{P}_i = 0, \quad (\text{A.11})$$

where

$$\mathcal{P}_2 = K, \quad (\text{A.12})$$

$$\mathcal{P}_3 = -2X(G_{3\phi} + \ddot{\phi}G_{3X}), \quad (\text{A.13})$$

$$\begin{aligned} \mathcal{P}_4 = & 2(3H^2 + 2\dot{H})G_4 - 4H^2X\left(3 + \frac{\dot{X}}{HX} + 2\frac{\dot{H}}{H^2}\right)G_{4X} \\ & - 8HX\dot{X}G_{4XX} + 2(\ddot{\phi} + 2H\dot{\phi})G_{4\phi} + 4XG_{4\phi\phi} + 4X(\ddot{\phi} - 2H\dot{\phi})G_{4\phi X}, \end{aligned} \quad (\text{A.14})$$

$$\begin{aligned} \mathcal{P}_5 = & -2X(2H^3\dot{\phi} + 2H\dot{H}\dot{\phi} + 3H^2\ddot{\phi})G_{5X} - 4H^2X^2\ddot{\phi}G_{5XX} \\ & + 4HX(\dot{X} - HX)G_{5\phi X} + 2H^2X\left(3 + 2\frac{\dot{X}}{HX} + 2\frac{\dot{H}}{H^2}\right)G_{5\phi} + 4HX\dot{\phi}G_{5\phi\phi}. \end{aligned} \quad (\text{A.15})$$

Here, $H = \dot{a}/a$ is the Hubble rate function and the dot means derivative with respect to time and ρ_{matter} and p_{matter} are the matter energy density and the pressure, respectively. The equation of motion of the scalar field is given by varying the action with respect to $\phi(t)$:

$$\frac{1}{a^3} \frac{d}{dt} (a^3 J) = P_\phi, \quad (\text{A.16})$$

where

$$\begin{aligned} J = & \dot{\phi}K_X + 6HXG_{3X} - 2\dot{\phi}G_{3\phi} + 6H^2\dot{\phi}(G_{4X} + 2XG_{4XX}) - 12HXG_{4\phi X} \\ & + 2H^3X(3G_{5X} + 2XG_{5XX}) - 6H^2\dot{\phi}(G_{5\phi} + XG_{5\phi X}), \end{aligned} \quad (\text{A.17})$$

$$\begin{aligned} P_\phi = & K_\phi - 2X(G_{3\phi\phi} + \ddot{\phi}G_{3\phi X}) + 6(2H^2 + \dot{H})G_{4\phi} + 6H(\dot{X} + 2HX)G_{4\phi X} \\ & - 6H^2XG_{5\phi\phi} + 2H^3X\dot{\phi}G_{5\phi X}. \end{aligned} \quad (\text{A.18})$$

Equations (A.6), (A.11), and (A.16) control the background evolution of the Universe. In the same manner as the quintessence model, Eqs. (A.11) and (A.16) are equivalent when Eq. (A.6) holds. Equations (A.6) and (A.11) can be rewritten in the well-known form

$$3H^2 = \kappa^2(\rho_{\text{matter}} + \rho_\phi), \quad (\text{A.19})$$

$$-3H^2 - 2\dot{H} = \kappa^2(p_{\text{matter}} + p_\phi), \quad (\text{A.20})$$

where we defined ρ_ϕ and p_ϕ as

$$\rho_\phi \equiv \sum_{i=2}^5 \mathcal{E}_i + \frac{3H^2}{\kappa^2}, \quad p_\phi \equiv \sum_{i=2}^5 \mathcal{P}_i - \frac{1}{\kappa^2}(3H^2 + 2\dot{H}). \quad (\text{A.21})$$

These equations define the effective energy density and effective pressure, respectively. As for the matter part, we may set $p_{\text{matter}} = 0$ as the pressures of both baryons and cold dark matter are negligible.

B Possibility of $\alpha < 0$

As mentioned in Sec. 4, a negative α can be realized in the case $G_{4\phi} \neq 0$ and $G_{3X} \neq 0$. To see this, we recapitulate the expression for α ,

$$\alpha = \frac{G_{4\phi}(2G_{4\phi} + \dot{\phi}^2 G_{3X})}{G_4 \left[K_X - 2G_{3\phi} + \ddot{\phi}(2G_{3X} + \dot{\phi}^2 G_{3XX}) + \dot{\phi}^2 G_{3\phi X} \right]}. \quad (\text{B.1})$$

Hence we have $\alpha < 0$ if we consider a model with $G_{4\phi}(2G_{4\phi} + \dot{\phi}^2 G_{3X}) < 0$, which may be realized by making $\dot{\phi}^2 G_{3X}$ the same order of $G_{4\phi}$. A simplest model would be to set $G_3 = -X/m^3$ and $K_X = 1$ with $m^3 \lesssim H_0^2 M_{pl}$. But we have not checked if this model could give an observationally viable model or not.

References

- [1] A. G. Riess, A. V. Filippenko, P. Challis, A. Clocchiatti, A. Diercks, P. M. Garnavich et al., *Observational Evidence from Supernovae for an Accelerating Universe and a Cosmological Constant*, *Astron. J.* **116** (1998) 1009 [[astro-ph/9805201](#)].
- [2] S. Perlmutter, G. Aldering, G. Goldhaber, R. A. Knop, P. Nugent, P. G. Castro et al., *Measurements of Ω and Λ from 42 High-Redshift Supernovae*, *Astrophys. J.* **517** (1999) 565 [[astro-ph/9812133](#)].
- [3] E. Komatsu, K. M. Smith, J. Dunkley, C. L. Bennett, B. Gold, G. Hinshaw et al., *Seven-year Wilkinson Microwave Anisotropy Probe (WMAP) Observations: Cosmological Interpretation*, *Astrophys. J. Suppl.* **192** (2011) 18 [[1001.4538](#)].
- [4] Planck Collaboration, P. A. R. Ade, N. Aghanim, C. Armitage-Caplan, M. Arnaud, M. Ashdown et al., *Planck 2013 results. XVI. Cosmological parameters*, *Astron. Astrophys.* **571** (2014) A16 [[1303.5076](#)].
- [5] Planck Collaboration, P. A. R. Ade, N. Aghanim, M. Arnaud, M. Ashdown, J. Aumont et al., *Planck 2015 results. XIII. Cosmological parameters*, *Astron. Astrophys.* **594** (2016) A13 [[1502.01589](#)].
- [6] D. J. Eisenstein, I. Zehavi, D. W. Hogg, R. Scoccimarro, M. R. Blanton, R. C. Nichol et al., *Detection of the Baryon Acoustic Peak in the Large-Scale Correlation Function of SDSS Luminous Red Galaxies*, *Astrophys. J.* **633** (2005) 560 [[arXiv:astro-ph/0501171](#)].
- [7] T. Okumura, T. Matsubara, D. J. Eisenstein, I. Kayo, C. Hikage, A. S. Szalay et al., *Large-Scale Anisotropic Correlation Function of SDSS Luminous Red Galaxies*, *Astrophys. J.* **676** (2008) 889 [[0711.3640](#)].
- [8] W. J. Percival, B. A. Reid, D. J. Eisenstein, N. A. Bahcall, T. Budavari, J. A. Frieman et al., *Baryon acoustic oscillations in the Sloan Digital Sky Survey Data Release 7 galaxy sample*, *Mon. Not. Roy. Astron. Soc.* **401** (2010) 2148 [[0907.1660](#)].

- [9] C. Blake, E. A. Kazin, F. Beutler, T. M. Davis, D. Parkinson, S. Brough et al., *The WiggleZ Dark Energy Survey: mapping the distance-redshift relation with baryon acoustic oscillations*, *Mon. Not. Roy. Astron. Soc.* **418** (2011) 1707 [[1108.2635](#)].
- [10] F. Beutler, C. Blake, M. Colless, D. H. Jones, L. Staveley-Smith, L. Campbell et al., *The 6dF Galaxy Survey: baryon acoustic oscillations and the local Hubble constant*, *Mon. Not. Roy. Astron. Soc.* **416** (2011) 3017 [[1106.3366](#)].
- [11] A. J. Cuesta, M. Vargas-Magaña, F. Beutler, A. S. Bolton, J. R. Brownstein, D. J. Eisenstein et al., *The clustering of galaxies in the SDSS-III Baryon Oscillation Spectroscopic Survey: baryon acoustic oscillations in the correlation function of LOWZ and CMASS galaxies in Data Release 12*, *Mon. Not. Roy. Astron. Soc.* **457** (2016) 1770 [[1509.06371](#)].
- [12] T. Delubac, J. E. Bautista, N. G. Busca, J. Rich, D. Kirkby, S. Bailey et al., *Baryon acoustic oscillations in the Ly α forest of BOSS DR11 quasars*, *Astron. Astrophys.* **574** (2015) A59 [[1404.1801](#)].
- [13] P. J. E. Peebles and B. Ratra, *Cosmology with a Time-Variable Cosmological “Constant”*, *Astrophys. J. Lett.* **325** (1988) L17.
- [14] B. Ratra and P. J. E. Peebles, *Cosmological consequences of a rolling homogeneous scalar field*, *Phys. Rev. D* **37** (1988) 3406.
- [15] T. Chiba, N. Sugiyama and T. Nakamura, *Cosmology with x -matter*, *Mon. Not. Roy. Astron. Soc.* **289** (1997) L5 [[astro-ph/9704199](#)].
- [16] I. Zlatev, L. Wang and P. J. Steinhardt, *Quintessence, Cosmic Coincidence, and the Cosmological Constant*, *Phys. Rev. Lett.* **82** (1999) 896 [[astro-ph/9807002](#)].
- [17] H. A. Buchdahl, *Non-linear Lagrangians and cosmological theory*, *Mon. Not. Roy. Astron. Soc.* **150** (1970) 1.
- [18] S. Nojiri and S. D. Odintsov, *Introduction to Modified Gravity and Gravitational Alternative for Dark Energy*, *arXiv e-prints* (2006) hep [[hep-th/0601213](#)].
- [19] T. P. Sotiriou and V. Faraoni, *$f(R)$ theories of gravity*, *Reviews of Modern Physics* **82** (2010) 451 [[0805.1726](#)].
- [20] A. De Felice and S. Tsujikawa, *$f(R)$ Theories*, *Living Reviews in Relativity* **13** (2010) 3 [[1002.4928](#)].
- [21] S. Nojiri and S. D. Odintsov, *Unified cosmic history in modified gravity: From $F(R)$ theory to Lorentz non-invariant models*, *Phys. Rept.* **505** (2011) 59 [[1011.0544](#)].
- [22] C. de Rham, G. Gabadadze and A. J. Tolley, *Resummation of Massive Gravity*, *Phys. Rev. Lett.* **106** (2011) 231101 [[1011.1232](#)].
- [23] S. F. Hassan and R. A. Rosen, *Resolving the Ghost Problem in Nonlinear Massive Gravity*, *Phys. Rev. Lett.* **108** (2012) 041101 [[1106.3344](#)].
- [24] S. F. Hassan and R. A. Rosen, *Bimetric gravity from ghost-free massive gravity*, *Journal of High Energy Physics* **2012** (2012) 126 [[1109.3515](#)].
- [25] G. W. Horndeski, *Second-Order Scalar-Tensor Field Equations in a Four-Dimensional Space*, *International Journal of Theoretical Physics* **10** (1974) 363.
- [26] V. Marra, L. Amendola, I. Sawicki and W. Valkenburg, *Cosmic Variance and the Measurement of the Local Hubble Parameter*, *Phys. Rev. Lett.* **110** (2013) 241305 [[1303.3121](#)].
- [27] A. G. Riess, L. M. Macri, S. L. Hoffmann, D. Scolnic, S. Casertano, A. V. Filippenko et al., *A 2.4% Determination of the Local Value of the Hubble Constant*, *Astrophys. J.* **826** (2016) 56 [[1604.01424](#)].
- [28] E. Di Valentino, A. Melchiorri and J. Silk, *Reconciling Planck with the local value of H_0 in extended parameter space*, *Physics Letters B* **761** (2016) 242 [[1606.00634](#)].
- [29] K. C. Wong, S. H. Suyu, G. C. F. Chen, C. E. Rusu, M. Millon, D. Sluse et al., *H0LiCOW XIII. A 2.4% measurement of H_0 from lensed quasars: 5.3 σ tension between early and late-Universe probes*, *arXiv e-prints* (2019) arXiv:1907.04869 [[1907.04869](#)].
- [30] G. C. F. Chen, C. D. Fassnacht, S. H. Suyu, C. E. Rusu, J. H. H. Chan, K. C. Wong et al., *A SHARP view of H0LiCOW: H_0 from three time-delay gravitational lens systems with adaptive optics imaging*,

Mon. Not. Roy. Astron. Soc. **490** (2019) 1743 [1907.02533].

- [31] S. Birrer, T. Treu, C. E. Rusu, V. Bonvin, C. D. Fassnacht, J. H. H. Chan et al., *H0LiCOW - IX. Cosmographic analysis of the doubly imaged quasar SDSS 1206+4332 and a new measurement of the Hubble constant*, Mon. Not. Roy. Astron. Soc. **484** (2019) 4726 [1809.01274].
- [32] I. Jee, S. H. Suyu, E. Komatsu, C. D. Fassnacht, S. Hilbert and L. V. E. Koopmans, *A measurement of the Hubble constant from angular diameter distances to two gravitational lenses*, Science **365** (2019) 1134 [1909.06712].
- [33] A. J. Shajib, S. Birrer, T. Treu, A. Agnello, E. J. Buckley-Geer, J. H. H. Chan et al., *STRIDES: A 3.9 per cent measurement of the Hubble constant from the strong lens system DES J0408-5354*, Mon. Not. Roy. Astron. Soc. (2020) [1910.06306].
- [34] L. Verde, T. Treu and A. G. Riess, *Tensions between the early and late Universe*, Nature Astronomy **3** (2019) 891 [1907.10625].
- [35] N. Kaiser, *Clustering in real space and in redshift space*, Mon. Not. Roy. Astron. Soc. **227** (1987) 1.
- [36] A. J. S. Hamilton, *Linear Redshift Distortions: a Review*, in *The Evolving Universe*, D. Hamilton, ed., vol. 231 of *Astrophysics and Space Science Library*, p. 185, (1998), DOI.
- [37] E. V. Linder, *Cosmic growth history and expansion history*, Phys. Rev. D **72** (2005) 043529 [arXiv:astro-ph/0507263].
- [38] B. Jain and P. Zhang, *Observational tests of modified gravity*, Phys. Rev. D **78** (2008) 063503 [0709.2375].
- [39] L. Guzzo, M. Pierleoni, B. Meneux, E. Branchini, O. Le Fèvre, C. Marinoni et al., *A test of the nature of cosmic acceleration using galaxy redshift distortions*, Nature **451** (2008) 541 [0802.1944].
- [40] Y.-S. Song and K. Koyama, *Consistency test of general relativity from large scale structure of the universe*, JCAP **1** (2009) 48 [0802.3897].
- [41] T. Okumura and Y. P. Jing, *Systematic Effects on Determination of the Growth Factor from Redshift-space Distortions*, Astrophys. J. **726** (2011) 5 [1004.3548].
- [42] C. Blake, S. Brough, M. Colless, C. Contreras, W. Couch, S. Croom et al., *The WiggleZ Dark Energy Survey: the growth rate of cosmic structure since redshift $z=0.9$* , Mon. Not. Roy. Astron. Soc. (2011) 834 [1104.2948].
- [43] L. Samushia, W. J. Percival and A. Raccanelli, *Interpreting large-scale redshift-space distortion measurements*, Mon. Not. Roy. Astron. Soc. **420** (2012) 2102 [1102.1014].
- [44] S. de la Torre, L. Guzzo, J. A. Peacock, E. Branchini, A. Iovino, B. R. Granett et al., *The VIMOS Public Extragalactic Redshift Survey (VIPERS) . Galaxy clustering and redshift-space distortions at $z\sim 0.8$ in the first data release*, Astron. Astrophys. **557** (2013) A54 [1303.2622].
- [45] B. A. Reid, H.-J. Seo, A. Leauthaud, J. L. Tinker and M. White, *A 2.5 per cent measurement of the growth rate from small-scale redshift space clustering of SDSS-III CMASS galaxies*, Mon. Not. Roy. Astron. Soc. **444** (2014) 476 [1404.3742].
- [46] Y.-S. Song, A. Taruya, E. Linder, K. Koyama, C. G. Sabiu, G.-B. Zhao et al., *Consistent modified gravity analysis of anisotropic galaxy clustering using BOSS DR11*, Phys. Rev. D **92** (2015) 043522 [1507.01592].
- [47] T. Okumura, C. Hikage, T. Totani, M. Tonegawa, H. Okada, K. Glazebrook et al., *The Subaru FMOS galaxy redshift survey (FastSound). IV. New constraint on gravity theory from redshift space distortions at $z \sim 1.4$* , Publ. Astron. Soc. Japan **68** (2016) 38 [1511.08083].
- [48] L. Kazantzidis and L. Perivolaropoulos, *Evolution of the $f\sigma_8$ tension with the Planck15 / Λ CDM determination and implications for modified gravity theories*, Phys. Rev. D **97** (2018) 103503 [1803.01337].
- [49] S. Nesseris, G. Pantazis and L. r. Perivolaropoulos, *Tension and constraints on modified gravity parametrizations of $G_{eff}(z)$ from growth rate and Planck data*, Phys. Rev. D **96** (2017) 023542 [1703.10538].
- [50] K. Koyama, *Structure formation in modified gravity models*, JCAP **2006** (2006) 017

[[astro-ph/0601220](#)].

- [51] S. A. Thomas, F. B. Abdalla and J. Weller, *Constraining modified gravity and growth with weak lensing*, *Mon. Not. Roy. Astron. Soc.* **395** (2009) 197 [[0810.4863](#)].
- [52] S. F. Daniel, E. V. Linder, T. L. Smith, R. R. Caldwell, A. Cooray, A. Leauthaud et al., *Testing general relativity with current cosmological data*, *Phys. Rev. D* **81** (2010) 123508 [[1002.1962](#)].
- [53] I. Tereno, E. Semboloni and T. Schrabback, *COSMOS weak-lensing constraints on modified gravity*, *Astron. Astrophys.* **530** (2011) A68 [[1012.5854](#)].
- [54] F. Simpson, C. Heymans, D. Parkinson, C. Blake, M. Kilbinger, J. Benjamin et al., *CFHTLenS: testing the laws of gravity with tomographic weak lensing and redshift-space distortions*, *Mon. Not. Roy. Astron. Soc.* **429** (2013) 2249 [[1212.3339](#)].
- [55] J. Matsumoto, *Oscillating solutions of the matter density contrast in Horndeski's theory*, *JCAP* **2019** (2019) 054 [[1806.10454](#)].
- [56] C. Schimd, J.-P. Uzan and A. Riazuelo, *Weak lensing in scalar-tensor theories of gravity*, *Phys. Rev. D* **71** (2005) 083512 [[astro-ph/0412120](#)].
- [57] W. Hu and I. Sawicki, *Models of $f(R)$ cosmic acceleration that evade solar system tests*, *Phys. Rev. D* **76** (2007) 064004 [[0705.1158](#)].
- [58] A. de Felice, T. Kobayashi and S. Tsujikawa, *Effective gravitational couplings for cosmological perturbations in the most general scalar-tensor theories with second-order field equations*, *Physics Letters B* **706** (2011) 123 [[1108.4242](#)].
- [59] J. O'Hanlon, *Intermediate-Range Gravity: A Generally Covariant Model*, *Phys. Rev. Lett.* **29** (1972) 137.
- [60] T. Chiba, *$1/R$ gravity and scalar-tensor gravity*, *Physics Letters B* **575** (2003) 1 [[astro-ph/0307338](#)].
- [61] C. Deffayet, X. Gao, D. A. Steer and G. Zahariade, *From k -essence to generalized Galileons*, *Phys. Rev. D* **84** (2011) 064039 [[1103.3260](#)].
- [62] T. Kobayashi, M. Yamaguchi and J. Yokoyama, *Generalized G -Inflation — Inflation with the Most General Second-Order Field Equations —*, *Progress of Theoretical Physics* **126** (2011) 511 [[1105.5723](#)].
- [63] B. P. Abbott, R. Abbott, T. D. Abbott, F. Acernese, K. Ackley, C. Adams et al., *GW170817: Observation of Gravitational Waves from a Binary Neutron Star Inspiral*, *Phys. Rev. Lett.* **119** (2017) 161101 [[1710.05832](#)].
- [64] B. P. Abbott, R. Abbott, T. D. Abbott, F. Acernese, K. Ackley, C. Adams et al., *Gravitational Waves and Gamma-Rays from a Binary Neutron Star Merger: GW170817 and GRB 170817A*, *Astrophys. J. Let.* **848** (2017) L13 [[1710.05834](#)].
- [65] B. P. Abbott, R. Abbott, T. D. Abbott, F. Acernese, K. Ackley, C. Adams et al., *Multi-messenger Observations of a Binary Neutron Star Merger*, *Astrophys. J. Let.* **848** (2017) L12 [[1710.05833](#)].
- [66] D. A. Coulter, R. J. Foley, C. D. Kilpatrick, M. R. Drout, A. L. Piro, B. J. Shappee et al., *Swope Supernova Survey 2017a (SSS17a), the optical counterpart to a gravitational wave source*, *Science* **358** (2017) 1556 [[1710.05452](#)].
- [67] C. Brans and R. H. Dicke, *Mach's Principle and a Relativistic Theory of Gravitation*, *Physical Review* **124** (1961) 925.
- [68] Y. Fujii and K.-I. Maeda, *The Scalar-Tensor Theory of Gravitation*. 2003.
- [69] J. Matsumoto, *Phantom crossing dark energy in Horndeski's theory*, *Phys. Rev. D* **97** (2018) 123538 [[1712.10015](#)].
- [70] S. Alam, M. Ata, S. Bailey, F. Beutler, D. Bizyaev, J. A. Blazek et al., *The clustering of galaxies in the completed SDSS-III Baryon Oscillation Spectroscopic Survey: cosmological analysis of the DR12 galaxy sample*, *ArXiv e-prints* (2016) [[1607.03155](#)].